Orig Life Evol Biosph (2016) 46:81–93
DOI 10.1007/s11084-015-9465-y

THEORETICAL MODELING

The Life Story of Hydrogen Peroxide III: Chirality and Physical Effects at the Dawn of Life

Rowena Ball[1] · **John Brindley**[2]

Received: 9 August 2015 / Accepted: 24 August 2015 /
Published online: 23 September 2015

Abstract It is a remarkable observed fact that all life on Earth is homochiral, its biology using exclusively the D-enantiomer of ribose, the sugar moiety of the ribonucleic acids, and the L-enantiomers of the chiral amino acids. Motivated by concurrent work that elaborates further the role of hydrogen peroxide in providing an oscillatory drive for the RNA world (Ball & Brindley 2015a, J. R. Soc. Interface 12, 20150366, and Ball & Brindley 2015b, this journal, in press), we reappraise the structure and physical properties of this small molecule within this context. Hydrogen peroxide is the smallest, simplest molecule to exist as a pair of non-superimposable mirror images, or enantiomers, a fact which leads us to develop the hypothesis that its enantiospecific interactions with ribonucleic acids led to enantioselective outcomes. We propose a mechanism by which these chiral interactions may have led to amplification of D-ribonucleic acids and extinction of L-ribonucleic acids.

Keywords Biological homochirality · RNA world · Hydrogen peroxide · Axial chirality

Introduction

The ubiquitous homochirality of biological molecules has puzzled and intrigued scientists and laypersons for generations. Its obvious interest and importance has motivated a vast literature on the whys, hows, mechanics and philosophical implications of the fact of

✉ Rowena Ball
Rowena.Ball@anu.edu.au

John Brindley
J.Brindley@leeds.ac.uk

[1] Mathematical Sciences Institute and Research School of Chemistry, The Australian National University, Canberra 2602, Australia

[2] School of Mathematics, University of Leeds, Leeds LS2 9JT, UK

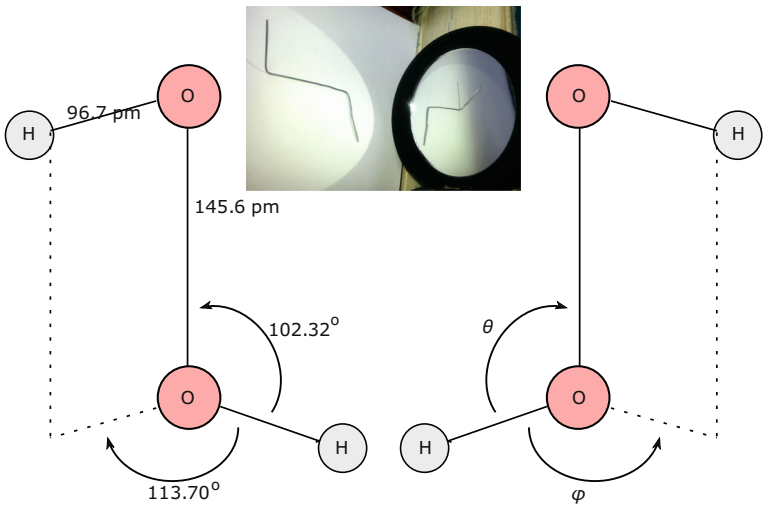

Fig. 1 Projections of 3-dimensional structural representations of the M *(left)* and P *(right)* enantiomers of hydrogen peroxide. θ is the bond angle, ϕ is the dihedral angle or angle between the two HOO planes. Inset: A model for the P enantiomer, which we fabricated, assiduously, in the office from a paper clip; its image reflected in the framed oval mirror is the M enantiomer, and a telltale shadow, just visible, in both cases betrays the out-of-plane OH bond

biological homochirality, and some of the multifarious schemes that have been proposed to explain its emergence are reviewed in Plasson et al. (2007), Blackmond (2011) and Ruiz-Mirazo and Briones (2014). Life on earth uses exclusively the D-enantiomer of ribose, the sugar moiety of the ribonucleic acids, and the L-enantiomers of the chiral amino acids. In Ball and Brindley (2014) and in parallel papers to this one (Ball and Brindley 2015a; 2015b) we have developed and tested the hypothesis that hydrogen peroxide was both the power source and agent for change in the pre-cellular RNA world, through its role as the THP (thiosulfate-hydrogen peroxide) oscillator providing the essential periodic thermal and pH drive. Here we focus on the structure and properties of hydrogen peroxide and review some of its pertinent physical properties in relation to its direct physicochemical role as an agent for the emergence and evolution of a living RNA world. In particular we propose that its chirality may have led to homochiral amplification of D-ribonucleic acids and extinction of the L species. This brief preliminary Report is purposely speculative and presents only preliminary results, intended to stimulate experimental studies to complement detailed mathematical and computational modelling work, currently underway in our group, aimed at elucidating in depth the processes described here. Since the context of our work is the pre-cellular RNA world, we focus on the ribonucleic acids rather than the amino acids.

Our key emphasis is that hydrogen peroxide is chiral in structure, too. It is the simplest such molecule, exhibiting axial chirality due to *trans* and *cis* potential barriers to internal rotation (Hunt et al. 1965), and thus existing as a pair of non-superimposable mirror images.[1] In normal bulk phase it occurs as a racemic mixture of the enantiomeric pair P (plus) and M (minus), which are represented in Fig. 1.

[1] Although all objects can have a mirror image (except for vampires of course!), only those for which their mirror images are non-superimposable are chiral.

There is also a high-quality literature concerned with the chirality of hydrogen peroxide, albeit exiguous. One strand involves fundamental theoretical studies of chiral discrimination in hydrogen-bonded (h-bonded) complexes of hydrogen peroxide with another chiral molecule (Dong et al. 2005; Du and Zhou 2006; Yin et al. 2009; Zhang et al. 2009). As reported by Churakov et al. (2009), crystals of L-serine perhydrate were prepared in which only one hydrogen peroxide enantiomer co-crystallized. These studies provide important evidence that hydrogen peroxide may interact enantiospecifically, but non-covalently, with chiral molecules in general. Experimental studies in which chiral organic peroxides were used for enantoselective epoxidations (Hoft 1993; Bunge et al. 2009; Bunge et al. 2013) provide evidence that covalent bonding interactions of chiral molecules with hydrogen peroxide can be enantiospecific and enantioselective.

Following Blackmond (2011), we define the enantiomeric excess ϕ for ribonucleotides and ribonucleic acids as

$$\phi = \frac{[\mathrm{D}] - [\mathrm{L}]}{[\mathrm{D}] + [\mathrm{L}]}$$

where the brackets denote concentrations. In this work we assume a symmetry-broken supply, i.e., $\phi_{\mathrm{supply}} \rightarrow 0^{+}$, and in "Through the Looking-Glass" section we outline a mechanism whereby ϕ may increase monotonically to 1, mediated by localised chiral microenvironments, illustrate a simplified version of the mechanism through a reinterpretation of the Frank (1953) model, and describe some of the flaws and pitfalls of dynamical system modelling of enantiomeric excess growth. In "The Medium is the Message" section we review relevant physical properties and discuss the possible effects on and consequences for the RNA world, and in "Summary and Outlook" section we summarize and anticipate work currently under way.

Through the Looking-Glass

To our knowledge enrichment of P or M enantiomers of hydrogen peroxide (Fig. 1) has not been achieved, or even attempted, in the bulk. This is because the activation energy for interconversion via the trans configuration is only 4617.6 J/mol (Hunt et al. 1965); it follows from the Boltzmann distribution that at 300 K 16 % of the population has energy greater than this, and the average energy of thermal fluctuations $\langle \delta E \rangle = \sqrt{C_{\mathrm{v}} k_b N_A T^2} \approx 7400\,\mathrm{J\,mol^{-1}}$, where C_{v} is the constant-volume molar heat capacity, k_b is the Boltzmann constant, and N_A is Avogadro's number. It is unlikely, too, that enantiomeric enrichment could be achieved at low temperature, because the quantum tunnelling time for interconversion is only 3×10^{-12} s (Bitencourt et al. 2008). Both thermal and quantum interconversion are expected to be effectively quenched when hydrogen peroxide forms tightly h-bonded complexes with other species and itself (Gao et al. 2010).

A racemic medium will be unable to enrich D or L nucleic acids in the bulk, but locally significant excesses of one hydrogen peroxide enantiomer are likely to occur, due to enantiopspecific interactions with the ribonucleotides and with itself (Alkorta et al. 2006). The hypothesis we develop here is based, with good supporting evidence, on the following assumptions:

1. A marginal excess of D-nucleotide precursors is fed to the system, due to some unspecified environmental asymmetry, which gives rise to a marginal excess of D-ribonucleic acids over L-ribonucleic acids, and chain length distributions with a small bias to D-chains of longer mean length than L-chains.

2. D and L species can interact via enantiomeric cross-inhibition of polymerisation (and therefore replication), as was shown experimentally by Joyce et al. (1984).
3. D- and L- ribonucleic acids experience localised enantiomeric excesses of hydrogen peroxide.
4. Effects of hydrogen peroxide on ribonucleic acids may be indirect, via conformational changes associated with h-bonding, and direct, via chemical oxidation.

Indirect Effects

The 2′-hydroxyl group is the key determinant of structure, function and reactivity of RNA (Acharya and Chattopadhyaya 2002; Fohrer et al. 2006). It is a crucial contributor to cooperative networks of hydrogen bonds (h-bonds) which stabilize helical secondary structure and folds such as tetraloops that are important for ribozyme activity. Since hydrogen peroxide is a stronger proton donor than water (Martins-Costa and Ruiz-López 2013), we propose that enantiospecific displacement of inter- or intramolecular proton donors by hydrogen peroxide at the 2′-hydroxyl group can disrupt RNA structural motifs.

Dong et al. (2005) obtained two pairs of optimized enantiomeric structures for h-bonded R and S lactic acid complexes with hydrogen peroxide, RP, SM, RM and SP, of which the significantly more stable pair was found to be RP and SM. By analogy, we propose that similar nucleotide complexes are DP, LM, DM and LP, and the more stable complexes are DP and LM. (This choice is arbitrary until settled by experiment.)

The L-ribonucleic acids are more destabilized by this chiral interaction than the D-ribonucleic acids, because the mean L-chain length is shorter, they are more likely to occur as single strands, and the L-2′-hydroxyl group is more likely to be exposed and less likely to be structurally protected. The D-ribonucleic acids are less susceptible, because the mean D-chain length is longer and the consequent greater capacity to form tightly h-bonded secondary structures would tend to protect the 2′-hydroxyl group.

Direct Interaction

There is strong experimental evidence that oxidation of nucleotides by hydrogen peroxide can occur directly, rather than by free OH radicals (Hofer 2001; Martins-Costa and Ruiz-López 2013). Thus it is reasonable to suppose that it can react enantiospecifically with ribonucleic acids.

With a greater fraction of L-chains over D-chains destabilized by indirect interaction, hydrogen peroxide can then ‘go in for the kill’, with one enantiomer (let us say M) preferentially oxidizing L-chains. Here we invoke the analogy of enantioselective epoxidations with chiral peroxides (Hoft 1993; Bunge et al. 2009; Bunge et al. 2013).

Of course, the shorter side of the D-chain distribution is also more destabilized and oxidised than the longer side, and the longer side of the L-chain distribution is better able to protect itself than the shorter side. But overall the process works in favour of increasing the average length of D-chains, up to a limit determined by thermal and pH cycling (Ball and Brindley 2015a), and decreasing that of L-chains.

The fraction of D-species increases over time, too, as well as the average length. However, the fraction of their enantiospecific reagent, P hydrogen peroxide, does not change! This gives rise to a subtle reinforcement effect: Since the racemic mixture persists in the bulk, due to facile P-M interconversion, the fraction c_D/c_P increases while the fraction c_L/c_M decreases over time. When $\phi = 1$ the destructive risk posed by hydrogen peroxide to a homochiral RNA world may be reduced by up to 50 %, in principle, over that to a racemic

RNA world. Although in reality this reduction would be lower, it would still be > 0. We see that as ϕ increases the RNA world becomes *fitter* with respect to its environment.

Thus emergence of homochirality *in itself* confers a significant advantage on replicating RNA species in a peroxide-mediated RNA world.

Modelling the Growth of Chirality from a Small Enantiomeric Excess

In terms of the well-known Frank model (Frank 1953) for development of a homochiral molecular system from a nearly racemic mixture, and many of its generalisations (e.g., (Kondepudi and Nelson 1984; Gutman et al. 1988; Gutman 2014)), the chiral interactions of nucleotides with hydrogen peroxide can be interpreted as reinforcing kinetically the effects of cross inhibition, thus accelerating the evolution of homochirality. Intuitively, any process that hastens homochiral development, especially in the early stages, is advantageous because there is more scope for the system dynamics to outpace large, rare fluctuations. This problem of large, stochastic fluctuations has been studied in the context of predicting times to population extinctions (Drummond et al. 2010; Ovaskainen and Meerson 2010). In a developing chiral system such fluctuations might otherwise keep the system see-sawing between relatively small D and L enantiomeric excesses.

Following Frank (1953) we assume that L and D enantiomers are produced autocatalytically from an infinite reservoir of non-chiral reagent. We assume further that L species are inactivated by the M enantiomer of hydrogen peroxide and D species are inactivated by the P enantiomer. We propose that the inactivation rate constant for L depends on the concentration of D, and that for D depends on the concentration of L. A physical argument for this effect is that since D is not affected (or less affected) by M it is more available to enhance the rate of inactivation of L by antagonism, and similarly, since L is less affected by P it is more available to enhance the rate of inactivation of D. This 'toy' reacting system is described as follows:

$$\mathrm{A} + \mathrm{D} \xrightarrow{k_1} 2\mathrm{D} \qquad \mathrm{A} + \mathrm{L} \xrightarrow{k_1} 2\mathrm{L} \tag{1}$$

$$\mathrm{L} + \mathrm{M} \xrightarrow{k_2(\mathrm{D})} \mathrm{Z} \qquad \mathrm{D} + \mathrm{P} \xrightarrow{k_2(\mathrm{L})} \mathrm{Z}, \tag{2}$$

where A is the non-chiral reagent, available in large excess, and Z is the inactivated product. The evolution of L and D is described by the following dynamical system:

$$\frac{\mathrm{d[D]}}{\mathrm{d}t} = k_1[\mathrm{A}][\mathrm{D}] - k_2[\mathrm{P}][\mathrm{L}][\mathrm{D}] = k_1'[\mathrm{D}] - k_2'[\mathrm{L}][\mathrm{D}] \tag{3}$$

$$\frac{\mathrm{d[L]}}{\mathrm{d}t} = k_1[\mathrm{A}][\mathrm{L}] - k_2[\mathrm{M}][\mathrm{D}][\mathrm{L}] = k_1'[\mathrm{L}] - k_2'[\mathrm{D}][\mathrm{L}], \tag{4}$$

where the inactivation rate constant k_2 has first order dependence on D or L, and the chiral forms P and M are in large excess and remain statistically equal in concentration due to rapid thermal interconversion. The enantioselective effects are present, but subsumed in the effective rate constant k_2'. The solution of Eqs. 3 and 4 can be found explicitly as

$$[\mathrm{D}](t) = [\mathrm{D}]_0([\mathrm{D}]_0 - [\mathrm{L}]_0)([\mathrm{D}]_0 - [\mathrm{L}]_0 Q)^{-1} e^{k_1' t} \tag{5}$$

$$[\mathrm{L}](t) = [\mathrm{L}]_0([\mathrm{D}]_0 - [\mathrm{L}]_0)([\mathrm{D}]_0 - [\mathrm{L}]_0 Q)^{-1} Q e^{k_1' t}, \tag{6}$$

where

$$Q \equiv \exp\left[-\frac{k_2'}{k_1'}\left([\mathrm{D}]_0 - [\mathrm{L}]_0\right) e^{k_1' t}\right].$$

(In writing (5) and (6) we have assumed an initial enantiomeric excess of D, $D_0 > L_0$.) Equations 5 and 6 tell us that for any enantiomeric excess of D, no matter how small, $\lim_{t\to\infty} L(t) = 0$. We also see that the larger the localised concentrations of M and P hydrogen peroxide, subsumed in k_2', the faster $L \to 0$.

We emphasize that the (Frank 1953) model and most of its variants including this simple model have heuristic value only, and show little verisimilitude to a real, experimentally accessible process. For one thing, Eqs. 5 and 6 predict $\lim_{t\to\infty} D(t) = \infty$! Nevertheless, the model is a useful starting point for more realistic modelling of the enantioselective effects of hydrogen peroxide on the early RNA world, currently underway by our group. This will include modelling enantioselective interactions of hydrogen peroxide with a polymerising RNA system, under the periodic thermal drive provided by the THP oscillator. Viedma and Cintas (2011) found that a homochiral solid phase emerged in boiling solutions containig a racemic mixture of chiral crystals, due to dissolution-crystallization cycling under a thermal gradient. An alternative cycling model has been proposed by Ribó et al. (2013), in which reactant flow circulates between two compartments, each maintained at a different constant temperature and within which, respectively, enantioselective and non-enantioselective reactive processes are enabled. These results suggest that the thermal cycles provided by the THP oscillator may play a role in inducing localised enantiomeric excesses of M and P hydrogen peroxide.

However, it is well to proceed cautiously, because more sophisticated dynamical models for enantiomeric enrichment can be structurally unstable, implying that they either contain some pathology or that they are missing important physics. As shown in Ball (2000), Ball (2001), and Ball and Haymet (2001) and references therein, this problem unfortunately is rather frequent in dynamical models for widely different systems. This makes it impossible to determine if different models, which appeal to the same physical phenomena (symmetry-breaking and enantiomeric enrichment, in our case), belong to the same qualitative universality class even though they may differ quantitatively, as is reasonably expected. Some earlier authors have derived dynamical models for enantiomeric enrichment, which are claimed to contain the symmetry-breaking pitchfork bifurcation (e.g., Ribó and Hochberg (2008)). Yet the pitchfork is a degenerate bifurcation, which is non-persistent to perturbation. The defining and non-degeneracy conditions for the pitchfork (which are not satisfied by equations 8 and 9 of Ribó and Hochberg (2008)) are given by Ball (2001)

$$G = G_x = G_{xx} = G_\lambda = 0, \quad G_{\lambda x} \neq 0, \quad G_{xxx} \neq 0, \tag{7}$$

where G is the bifurcation equation for the steady states of the dynamical system, obtained in terms of a selected state variable x (sometimes implicitly), the bifurcation parameter of choice λ and the other parameters of the system. The normal form for the pitchfork — i.e., the simplest bifurcation equation that satisfies conditions (7), is

$$G(x, \lambda) = \pm x^3 \pm \lambda x. \tag{8}$$

It can be seen that any system containing a pitchfork must contain an effective cubic nonlinearity. However, Eq. 8 is degenerate, and structurally fragile to small perturbation. Two more parameters are needed to unfold it smoothly. A universal unfolding of the pitchfork is given by

$$G(x, \lambda, \alpha, \beta) = x^3 - \lambda x + \alpha + \beta x^2. \tag{9}$$

The parameter α is symmetry-breaking and its sign will determine the sign of x towards which the pitchfork will dissolve. In any model of a real dynamical system that contains a pitchfork α must always be nonzero (Ball 2001). The parameter β is the coefficient of the

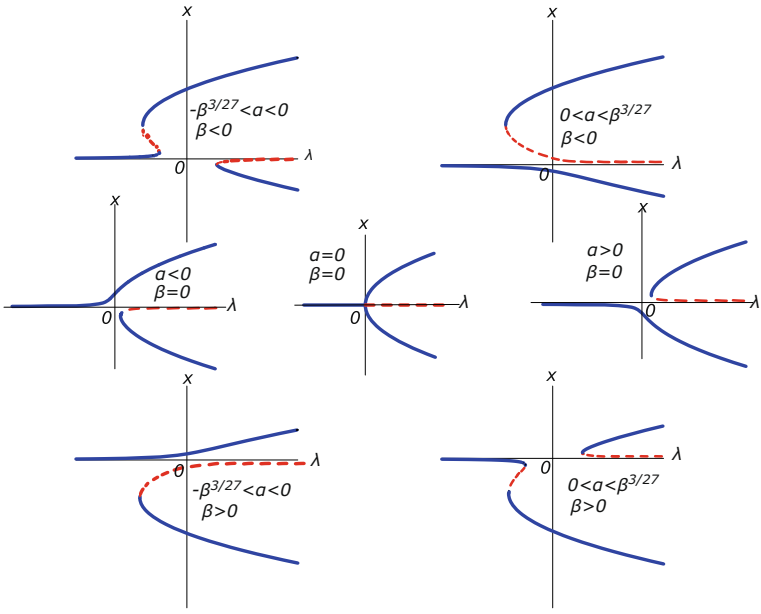

Fig. 2 The four qualitatively distinct bifurcation diagrams from the universal unfolding of the pitchfork Eq. 9 — *top left, top right, bottom left, bottom right*. The bifurcation diagram for the pitchfork normal form Eq. 8 is shown centre, flanked left and right by the two partial unfoldings

quadratic term in Eq. 9 and it tells us that the hysteresis bifurcation must also be present. In Fig. 2 are sketched the twice-degenerate pitchfork (centre), the four qualitatively distinct bifurcation diagrams of the universal unfolding (9), and the two partial unfoldings. (A miror-image set of bifurcation diagrams may also be constructed.)

If we interpret Eq. 9 as the normal form corresponding to the right hand sides of a dynamical model for enantiomeric enrichment of x, where is x identified with the enantiomeric excess ϕ, the bifurcation diagrams in Fig. 2 suggest some potentially interesting scenarios. The racemic state is $x = 0$ but in all physical situations α is nonzero (but small) and symmetry is broken. In the top left and lower right bifurcation diagrams the symmetry-broken steady states $(\pm x, \lambda)$ must undergo an abrupt jump to a highly non-racemic — but not necessarily homochiral — state at a turning point when the system is still only marginally non-racemic. If, at this upper steady state, the parameter λ continues to increase quasistatically, the system continues to become more highly non-racemic, and homochirality is possible. The bifurcation diagrams top right and lower left of Fig. 2 disallow jumps to high non-racemic states at a stability change — but they do permit collapse of a highly non-racemic state to an almost-racemic state! We emphasize that in a system for which the highest order steady-state singularity is a pitchfork, the bifurcation diagrams in Fig. 2 illustrate *all* of the qualitatively distinct behavours of which it is capable.

In a structurally stable model for symmetry-broken evolution of enantiomeric excess, the parameter λ may be qualitatively equivalent to a flow coefffcient, bringing reactants into a reacting volume and taking reactants and products out of the volume. (The diagrams may be translated into the positive realm by appropriate transformations.) The parameter α may be identified with a symmetry-broken enantiomeric excess ϕ_{f} brought in by the flow. β is the rate coefficient for a quadratic term. The coefficient of the cubic term is subsumed into λ,

α and β. Cubic nonlinearities can occur in chemical systems (e.g., Ball and Haymet 2001), but they can be rather artificial, requiring two-timing assumptions on some of the chemical rate terms to be incorporated into the model, and they tend to dissolve in a more detailed treatment.

In our experience, the simplest physical mechanism for obtaining an effective, robust cubic nonlinearity that fulfils the conditions (7) is to incorporate an enthalpy balance so that the temperature becomes a dynamical variable, coupled to the concentrations via the Arrhenius temperature-dependence of the rate constants (Ball 2001; Ball et al. 2004). The enthalpy balance is coupled to a heat bath at constant temperature and the specific heat and reaction enthalpies, to a good approximation, are constant. The extreme nonlinearity of the exponential temperature dependence of the reaction rates elicits the pitchfork (and higher order bifurcations) under relatively mild conditions. In such systems, there are, also, in most cases, Hopf bifurcations present, which could make for interesting interpretation! The price is greater computational and benchmarking difficulty, but we feel the result would be more natural, since it does not require artificial cubic chemistry and a temperature-varying environment would be the norm for the RNA world — we must presume it did not grow and prosper at 298 K exactly, always.

Detailed modelling and simulations are underway in our group, as intimated above, of the role of hydrogen peroxide in the development of enantiomeric excesses of nucleic acids based on the principles outlined here of ensuring the structural stability of the model and using the temperature as a dynamical variable.

The Medium is the Message

The philosopher Marshall McLuhan (http://en.wikipedia.org/wiki/Marshall_McLuhan) proposed that society is affected by the intrinsic properties of a medium, rather than by the information the medium carries. 'Medium' is understood in a broad sense; here the medium is hydrogen peroxide in solution and the 'society' on which it operates is the RNA population. In this section we discuss how the physical properties tabulated in Table 1 may have helped to structure the RNA world, considering the entries in ordered point form:

- Phase equilibrium and colligative effects:

  The freezing point depression ΔT_f and boiling point elevation ΔT_b adds to that induced by other solutes present, since

  $$\Delta T_\mathrm{f} = K_\mathrm{f}(m_1 + m_2 + \ldots + m_n) \quad \text{and} \quad \Delta T_\mathrm{b} = K_\mathrm{b}(m_1 + m_2 + \ldots + m_n),$$

  where K_f and K_b are the respective constants and $m_1 \ldots m_n$ are solute molalities. We may envisage hydrogen peroxide as playing a more-or-less significant part in broadening the temperature range of the liquid phase for the RNA world.

  The decrease in vapor pressure with increasing hydrogen peroxide concentration indicates a considerably lower volatility than that of pure water, as does the higher heat of vaporization. These properties may effect a concentration mechanism.
- Density:

  Coupling between the Soret effect and convection, proposed by Mast et al. (2011) as a mechanism for concentrating ribonucleotides and RNA and driving polymerisation of longer chains, may be affected by the higher density of hydrogen peroxide solutions in opposing ways:

Table 1 Relevant physical properties of hydrogen peroxide, solutions and pure (wt%), compared with those for pure water (second column) (Schumb et al. 1953; Gubskaya and Kusalik 2002; Martins-Costa and Ruiz-López 2013; McGrath 2015)

	0	5 %	10 %	50 %	100 %
Freezing point (°C)	0		−2.9	−6.4	
Boiling point (°C, 1 atm)	100		103	112	
Total vapor pressure (kPa, 25 °C)	3.16	2.99	2.81	1.22	0.26
Heat of vaporization (kJ/mole, 25 °C)	40.86				51.61
Density (g/ml, 25 °C)	0.9971	1.0145	1.0324	1.1914	1.4425
Viscosity (mPa s, 20 °C)	1.005		1.011	1.170	1.249
Surface tension (mN/m, 20 °C)	72.75		73.18	75.68	80.4
Diffusion coefficient (cm^2/day)	1.80	1.03[a]			
Dielectric constant (0 °C)	88.0	(See text.)			84.9
Permanent dipole moment (D)	2.95	2.56[b]			1.75[c]
Electronic polarizability (cm^3/mol)	0.885				1.39

[a]computed, in 0.68 % solution,

[b]in 0.36 % solution,

[c]vapor

- Since the particle thermophoretic velocity is inversely proportional to the fluid density $\rho(T)$ (Brenner and Bielenberg 2005), thermophoresis would be slowed.
- In the dynamic thermochemical environment proposed in Ball and Brindley (2015a), thermal cycling and concentration fluctuations of hydrogen peroxide could manifest as relatively strong density gradients. Since the driver of thermophoretic motion is actually the density gradient (Brenner and Bielenberg 2005), thermophoresis would be enhanced.

- Viscosity and surface tension:

  A small surfactant effect of hydrogen peroxide may provide a a favourable environment for vesicles or proto-cells to form, given a supply of phospholipids or simpler amphiphiles. Increased visosity is likely to encourage vesicle division in a dynamic environment, due to shear stresses (Zhu and Szostak 2009). The effects would be small, but the advantages of enclosure within a semi-permeable membrane are so great for biological molecules and processes that selection pressure would be strong to evolve catalytic replication, and reduce reliance on thermochemical cycling to melt double-stranded RNA (Ball and Brindley 2014), which would tend to disrupt primitive membranes.

  Thus, the dynamic presence of hydrogen peroxide can effectively prepare the RNA world for continued existence and evolution as the supply diminishes.
- Electrical properties:

  Relative permittivity data for hydrogen peroxide solutions are very interesting indeed, with respect to chiral discrimination, because this property shows a maximum that shifts to higher concentrations with decreasing temperature as shown in Fig. 3. This anomalous maximum was attributed to enhanced structuring of water (Gross

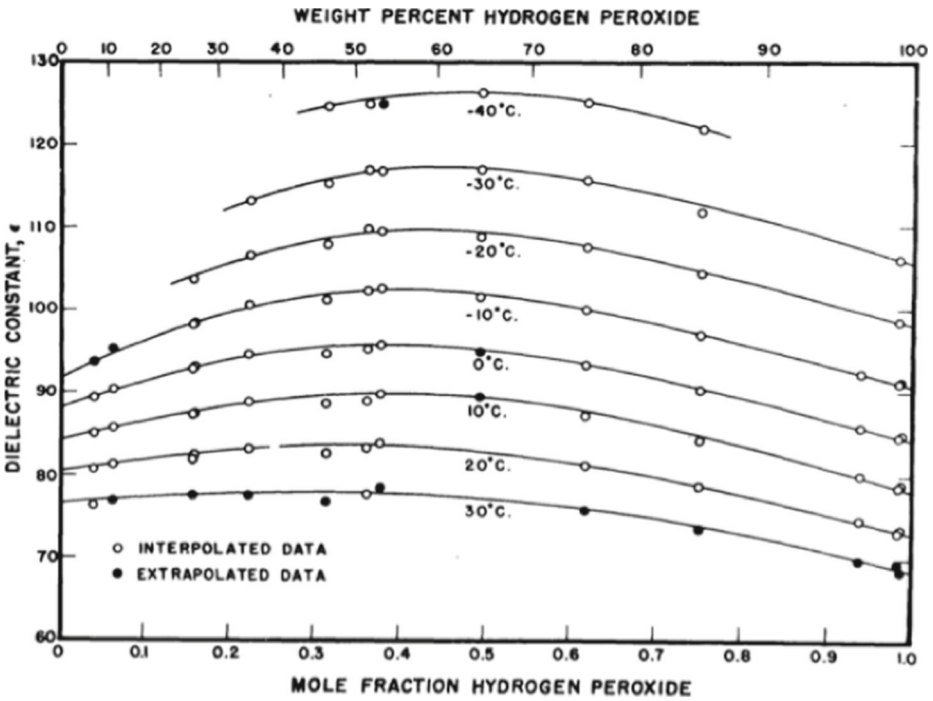

Fig. 3 Relative permittivity-composition isotherms for hydrogen peroxide-water solutions, from Gross and Taylor (1950). Under the experimental conditions the solutions are supercooled

and Taylor 1950), but in the light of more recent quantum mechanical calculations (Alkorta et al. 2006) it may be due more to the aggregation of homochiral and heterochiral clusters. From these data, using the Debye equation and assuming constant density, we can calculate the mean dipole moment of a 0.5 mole fraction solution as $\mu \approx 6.0\,\mathrm{D}$. While, strictly speaking, the dipole moment is a molecular property, this result does provide evidence that hydrogen peroxide solutions are more polar, h-bonded, and highly structured than pure water, especially given that the computed dipole moment for unstructured hydrogen peroxide in solution is only 2.56 D (Table 1). Enantiospecific interactions with the 2′-OH group of the ribonucleotides would tend to stabilise homochiral clusters and provide the localised chiral environment that leads ulimately to D-amplification.

Summary and Outlook

We have sketched an animated hypothetical picture, based on known chiral interactions of hydrogen peroxide and substituted peroxides with axial chirality, in which enantiospecific interactions of hydrogen peroxide with an almost-chiral RNA world preferentially select a D-RNA population that becomes progressively fitter in that environment, but have the opposite effect on the L population. Although these effects are small, as they must be,

because large perturbations are more likely to wipe out life, or incipient life, than mediate and enhance it, their ultimate consequence can be the elimination of the L-population. In developing and deepening this picture, of course the devil will be in the detail. Detailed dynamical modelling currently underway by our group is based on the evolution of interacting, length-structured populations — i.e., population distributions, adapting a methodology that was developed by Diekmann et al. (1998) and furthered by Clother and Brindley (2000) for modelling physiologically structured populations, using temperature dependent rate constants and incorporating an enthalpy balance.

Our review of the physical properties of hydrogen peroxide suggests that its effects may be favourable in terms of mediating the RNA world.

The wide interest in the topic of this research may help explain the persistence in human cultures of vampire myths — when one reflects on it, or attempts to, as it were, in a sense we are all vampires, made of molecules that have no natural mirror images on this world, forever searching the universe for our mirror image alien counterparts . . .

Acknowledgments This work was supported by Australian Research Council Future Fellowship FT0991007 (Rowena Ball).

References

Acharya P, Chattopadhyaya J (2002) The hydrogen bonding and hydration of 2′-OH in adenosine and adenosine 3′-ethyl phosphate. J Organic Chem 67:1852–1865. doi:10.1021/jo010960j

Alkorta I, Zborowski K, Elguero J (2006) Self-aggregation as a source of chiral discrimination. Chem Phys Lett 427:289–294. doi:10.1016/j.cplett.2006.06.104

Ball R (2000) Singularity theory study of overdetermination in models for l–h transitions. Phys Rev Lett 84:71–75. doi:10.1103/PhysRevLett.84.3077

Ball R (2001) Understanding critical behaviour through visualization: A walk around the pitchfork. Comput Phys Commun 142:3077–3080. doi:10.1016/S0010-4655(01)00322-8

Ball R, Brindley J (2014) Hydrogen peroxide thermochemical oscillator as driver for primordial RNA replication. J Roy Soc Interface 11:20131,052. doi:10.1098/rsif.2013.1052

Ball R, Brindley J (2015a) The life story of hydrogen peroxide II. A periodic pH thermochemical drive for the RNA world. J Roy Soc Interface 12:20150366. doi:10.1098/rsif.2015.0366

Ball R, Brindley J (2015b) Thiosulfate-hydrogen peroxide redox oscillator as pH driver for ribozyme activity in the RNA world. Origins of Life and Evolution of Biospheres, in press. doi:10.1007/s11084-015-9448-z

Ball R, Haymet ADJ (2001) Bistability and hysteresis in self-assembling micelle systems: phenomenology and deterministic dynamics. Phys Chem Chem Phys 3:4753–4761. doi:10.1039/b104483b

Ball R, McIntosh AC, Brindley J (2004) Feedback processes in cellulose thermal decomposition. Implications for fire-retarding strategies and treatments. Combust Theor Model 8:281–75. doi:10.1088/1364-7830/8/2/005

Bitencourt ACP, Ragnil M, Maciel GS, Aquilanti V, Prudente FV (2008) Level distributions, partition functions, and rates of chirality changing processes for the torsional mode around O-O bonds. J Chem Phys 129:154,316. doi:10.1063/1.2992554

Blackmond DG (2011) The origin of biological homochirality. Phil Trans Roy Soc B 366:2878–2884. doi:10.1098/rstb.2011.0130

Brenner H, Bielenberg JR (2005) A continuum approach to phoretic motions: Thermophoresis. Physica A 355:251–273. doi:10.1016/j.physa.2005.03.020

Bunge A, Hamann HJ, McCalmont E, Liebscher J (2009) Enantioselective epoxidation of 2-substituted 1,4-naphthoquinones using gem-dihydroperoxides. Tetrahedron Lett 50:4629–4632. doi:10.1016/j.tetlet.2009.05.096

Bunge A, Hamann HJ, Dietza D, Liebscher J (2013) Enantioselective epoxidation of tertiary allylic alcohols by chiral dihydroperoxides. Tetrahedron 69:2446–2450. doi:10.1016/j.tet.2013.01.032

Churakov AV, Prikhodchenko PV, Howard JAK, Lev O (2009) Glycine and L-serine crystalline perhydrates. Chem Commun 28:4224–4226. doi:10.1039/b906801e
Clother DR, Brindley J (2000) Stochastic development of individual members of a population: a Brownian motion approach. Bull Math Biol 62:1003–1034. doi:10.1006/bulm.2000.0189
Diekmann O, Gyllenberg M, Metz JAJ, Thieme HR (1998) On the formulation and analysis of general deterministic structured population models — I. Linear theory. J Math Biol 36:349–388. doi:10.1007/s002850050104
Dong XL, Zhoua ZY, Liua SZ, Gonga XL (2005) Theoretical study of chiral discrimination in the hydrogen bonding complexes of lactic acid and hydrogen peroxide. J Molecular Structure: THEOCHEM 718:9–15. doi:10.1016/j.theochem.2004.10.053
Drummond PD, Vaughan TG, Drummond AJ (2010) Extinction times in autocatalytic systems. J Phys Chem A 114:10,481–10,491. doi:10.1021/jp104471e
Du D, Zhou Z (2006) Chiral discrimination in hydrogen-bonded complexes of hydrogen peroxide with methyl hydroperoxide: Theoretical study. Int J Quantum Chem 106:935–942. doi:10.1002/qua.20790
Fohrer J, Hennig M, Carlomagno T (2006) Influence of the 2-hydroxyl group conformation on the stability of A-form helices in RNA. J Molecular Biol 356:280–287. doi:10.1016/j.jmb.2005.11.043
Frank FC (1953) On spontaneous asymmetric synthesis. Biochim Biophys Acta 11:459–463. doi:10.1016/0006-3002(53)90082-1
Gao H, Zhang G, Meng L, Chen D (2010) Chiral discrimination in hydrogen-bonded complexes of 2-fluorooxirane with hydrogen peroxide. Mol Phys 108:2073–2080. doi:10.1080/00268976.2010.505207
Gross PM, Taylor RC (1950) The dielectric constants of water, hydrogen peroxide and hydrogen peroxide-water mixtures. J Am Chem Soc 72:2075–2080. doi:10.1021/ja01161a055
Gubskaya AV, Kusalik PG (2002) The total molecular dipole moment for liquid water. J Chem Phys 117:5290–5302. doi:10.1063/1.1501122
Gutman I (2014) Frank model with limited resources. J Math Chem 52:2330–2333. doi:10.1007/s10910-014-0388-z
Gutman I, Babović V, Jokić S (1988) The origin of biomolecular chirality: The generalized Frank model with arbitrary initial conditions. Chem Phys Lett 144:187–190. doi:10.1016/0009-2614(88)87114-8
Hofer T (2001) Oxidation of 2-deoxyguanosine by H_2O_2-ascorbate: evidence against free OH and thermodynamic support for two-electron reduction of H_2O_2. J Chem Soc Perkin Trans 2(2):210–213. doi:10.1039/B006394K
Hoft E (1993) Enantioselective epoxidation with peroxidic oxygen. Top Curr Chem 164:63–77
Hunt RH, Leacock RA, Peters CW, Hecht KT (1965) Internal rotation in hydrogen peroxide: The far infrared spectrum and the determination of the hindering potential. J Chem Phys 42:1931–1946. doi:10.1063/1.1696228
Joyce GF, Visser GM, van Boeckel CAA, van Boom JH, Orgel LE, van Westrenen J (1984) Chiral selection in poly(C)-directed synthesis of oligo(G). Nature 310:602–604. doi:10.1038/310602a0
Kondepudi DK, Nelson GW (1984) Chiral-symmetry-breaking states and their sensitivity in nonequilibrium chemical systems. Physica A: Stat Mech Appl 125:465–496. doi:10.1016/0378-4371(84)90065-7
Martins-Costa MTC, Ruiz-López MF (2013) Molecular dynamics of hydrogen peroxide in liquid water using a combined quantum/classical force field. Chem Phys 332:341–347. doi:10.1016/j.chemphys.2006.12.018
Mast CB, Schink S, Gerland U, Braun D (2011) Escalation of polymerization in a thermal gradient. Proc Natl Acad Sci 110:8030–8035. doi:10.1073/pnas.1303222110
McGrath MP (2015) Torsional electric dipole moment functions calculated for HOOH and ClOOCl. J Chem Phys 138:094,305. doi:10.1063/1.4792364
Ovaskainen O, Meerson B (2010) Stochastic models of population extinction. Trends Ecol Evol 25:643–652. doi:10.1016/j.tree.2010.07.009
Plasson R, Kondepudi DK, Bersini H, Commeyras A, Asakura K (2007) Emergence of homochirality in far-from-equilibrium systems: Mechanisms and role in prebiotic chemistry. Chirality 19:589–600. doi:10.1002/chir.20440
Ribó JM, Hochberg D (2008) Stability of racemic and chiral steady states in open and closed chemical systems. Phys Lett A 373:111–122. doi:10.1016/j.physleta.2008.10.079
Ribó JM, Crusats J, el Hachemi Z, Moyano A, Blanco C, Hochberg D (2013) Spontaneous mirror symmetry breaking in the limited enantioselective autocatalysis model: Abyssal hydrothermal vents as scenario for the emergence of chirality in prebiotic chemistry. Astrobiology 13:132–142. doi:10.1089/ast.2012.0904
Ruiz-Mirazo K, Briones C (2014) de la Escosura A. Prebiotic systems chemistry: New perspectives for the origins of life. Chem Rev 114:285–366. doi:10.1021/cr2004844
Schumb WC, Satterfield CN, Wentworth RL (1953) Hydrogen Peroxide. Tech. Rep. 43, Part Two, 232 pp, Massachusetts Institute of Technology, Cambridge, Mass

Viedma C, Cintas P (2011) Homochirality beyond grinding: deracemizing chiral crystals by temperature gradient under boiling. Chemical Communications 47:12,786–12,788. doi:10.1039/C1CC14857E
Yin A, Zhang G, Chen D (2009) Chiral discrimination in hydrogen-bonded complexes of butan-2-ol (m-form) and hydrogen peroxide. Int J Quantum Chem 109:1472–1480. doi:10.1002/qua.21974
Zhang G, Yin A, Chen D (2009) Chiral discrimination in hydrogen-bonded complexes of 2-methylol oxirane with hydrogen peroxide. Int J Quantum Chem 109:920–930. doi:10.1002/qua.21878
Zhu TF, Szostak JW (2009) Coupled growth and division of model protocell membranes. J Am Chem Soc 131:5705–5713. doi:10.1021/ja900919c